Pallidotomy Increases Activity of Motor Association Cortex in Parkinson's Disease: A Positron Emission Tomographic Study

Scott T. Grafton, MD,*† Cheryl Waters, MD,* James Sutton, MD,* Mark F. Lew, MD,* and William Couldwell, MD‡

Stereotactic posteroventral pallidotomy can improve motor performance in Parkinson's disease. Interruption of inhibitory pallidal projections to ventrolateral thalamus, components of a cortical–basal ganglia motor loop allows for this clinical benefit. We hypothesized that pallidotomy would lead to increased movement related activity in motor cortical areas receiving projections from ventrolateral thalamus. This was tested in 6 Parkinson's disease patients who underwent stereotactic posteroventral pallidotomy. Each patient was imaged with positron emission tomography (PET) measures of regional cerebral blood flow (rCBF) during performance of a simple prehension task and at rest. Scans were acquired before and 17 weeks after surgery. After pallidotomy, movement-related changes of rCBF increased significantly in both the supplementary motor area (SMA) and premotor cortex but not in primary motor cortex. The results demonstrate the importance of pallidothalamic circuitry for regulating volitional movements and confirm that disruption of inhibitory input to the ventrolateral thalamus can augment movement-related activity in motor association areas.

Grafton ST, Waters C, Sutton J, Lew MF, Couldwell W. Pallidotomy increases activity of motor association cortex in Parkinson's disease: a positron emission tomographic study. Ann Neurol 1995;37:776–783

Pathologic changes in idiopathic Parkinson's disease (PD) include a marked loss of nigrostriatal dopaminergic neurons, resulting in clinical manifestations of bradykinesia, tremor, rigidity, and postural changes. Previous positron emission tomographic (PET) and single-photon emission computed tomographic (SPECT) imaging studies of patients with PD demonstrate a reduction of movement related cerebral activity in the supplementary motor area (SMA), rather than the basal ganglia [1, 2]. These attenuated responses at the level of the mesial frontal cortex may be a consequence of abnormal basal ganglia modulation of thalamocortical activity. In a cortical–basal ganglia model proposed by Alexander and colleagues [3], nigrostriatal dopamine deficiency leads to a decrease of inhibitory activity from putamen to the internal segment of the globus pallidus. Concomitant preservation of excitatory subthalamic projections would result in unchecked pallidal inhibition of the ventrolateral thalamus, culminating in reduced thalamocortical activity and depressed motor cortical activity. A network diagram highlighting these motor systems interactions in PD is shown in Figure 1. Direct evidence in support for this functional network has emerged from nonhuman primate l-methyl-4-phenyl-1,2,3,6-tetrahydropyridine (MPTP) models of parkinsonism [4–7]. Single unit recordings in human globus pallidus are also consistent with this model [8]. Furthermore, human PET and SPECT studies show that treatment with dopamine agonists increases movement-related activity in the SMA region [2, 9].

Stereotactic pallidotomy improves bradykinesia in selected patients with PD, presumably by reducing inhibitory pallidothalamic activity [10]. This should result in increased thalamocortical interactions and increased movement-related activity in motor cortical areas (including SMA). To test this hypothesis, we measured regional cerebral blood flow (rCBF) during movement and at rest in 6 patients with advanced PD. Each patient was studied before and after unilateral pallidotomy. A network analysis of interregional interactions was previously reported in a subset of this patient population [11].

Materials and Methods

Subjects

Six patients with idiopathic PD participated in the study after informed consent was obtained in accordance with the Insti-

From the Departments of *Neurology, †Radiology, and ‡Neurosurgery, University of Southern California, Los Angeles, CA.

Received Dec 5, 1994, and in revised form Feb 17, 1995. Accepted for publication Feb 22, 1995.

Address correspondence to Dr Grafton, Department of Neurology, USC, HCC 350, 1510 San Pablo Street, Los Angeles, CA 90033-4606.

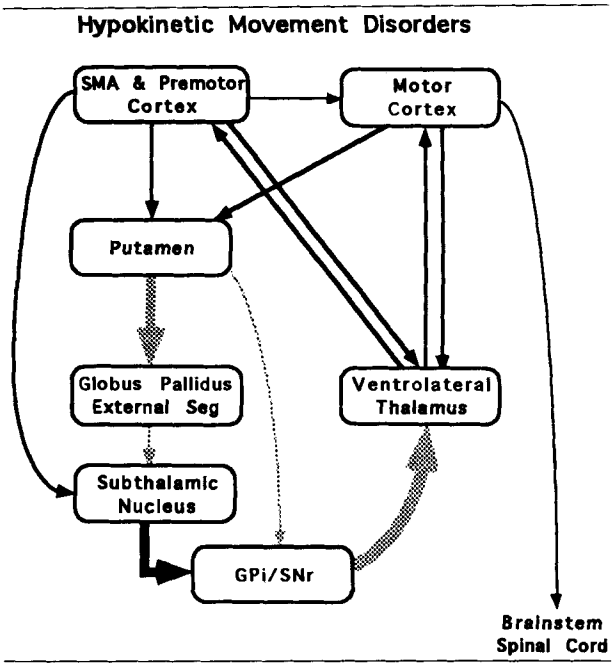

Fig 1. Cortical–subcortical motor loop in Parkinson's disease. Excitatory connections are shown in black, inhibitory inputs are in gray. Dopamine deficiency in the putamen leads to unbalanced activity from subthalamic nucleus into globus pallidus, resulting in pallidothalamic inhibition. Posteroventral pallidotomy interrupts inhibitory pallidal output. SMA = supplementary motor area; GPi = globus pallidus pars interna; Seg = segment; SNr = substantia nigra pars reticulata.

tutional Review Board of the University of Southern California. Five were right-handed and 1 was left-handed as determined with a standardized inventory [12]. None had clinical or radiographic evidence of dementia or other neurologic abnormalities at enrollment. Clinical features for each individual are summarized in Table 1. The mean age was 63 years and average disease duration was 13 years. The mean Hoehn and Yahr scores were 3.8 "off" and 3.3 "on." One subject (Patient 6) had a previous stereotactic thalamotomy 15 years previously in the hemisphere opposite to the planned pallidotomy.

Study Protocol

After completing a clinical evaluation and baseline PET studies, patients underwent computed tomographic (CT) guided unilateral posteroventral pallidotomy in the hemisphere opposite to their dominant hand as described previously [10]. The Cosman-Roberts-Wells stereotactic instrument was used [13]. The initial target was 2 mm anterior to the midpoint between the anterior and posterior commissure (AC-PC line), 19 to 22 mm lateral to the AC-PC line and 5 mm ventral to the AC-PC line. Patients were awake during the procedure. Optimal positioning was determined by testing each patient's response to electrical stimulation. Stimulation was administered through a monopole electrode at 2 to 5 Hz and at higher frequencies, 50 Hz. Patients were assessed for visual hallucinations, suggesting optic tract involvement. Evidence for clonic, tonic, or dystonic movements of the extremities or face and speech changes were evaluated. If the latter were present, then a temporary lesion was placed by heating to only 42°C. In most cases, a reversible improvement of motor performance was apparent. Then a permanent lesion was made by heating to 72 to 80°C for up to 60 seconds. The electrode was moved in 2-mm increments and heating was repeated to increase the overall lesion size. The total number of lesions was determined by intraoperative clinical response.

Repeat functional PET imaging was obtained an average of 17 weeks postoperatively. Patients were off all medications for at least 12 hours prior to pre- and postoperative PET imaging. Anatomic magnetic resonance imaging (MRI) studies were obtained 3 to 6 days after pallidotomy for lesion localization and coregistration with PET functional results.

Neurobehavioral Tasks

Patients lay supine in the PET scanner with their head immobilized with a foam head restraint (Smithers Corp, Akron, OH). They performed a movement task and a rest condition with the hand contralateral to the pallidotomy [14]. In the movement task, subjects reached and grasped cylindrical tar-

Table 1. Clinical Summary and Pallidotomy Localization

						Posteroventral Pallidotomy			
				Hoehn & Yahr		Stereotactic Coordinates		*y* Distance to Mid	Vertical Extent
Subject	Sex	Age (yr)	Disease Duration (yr)	On	Off	*x*	*y*	AC-PC Point	of Lesion
1	M	69	14	1.5	2.5	21	−8	3	1.5 to −3
2	M	64	5	5.0	5.0	17	−9	5	6 to −3
3	F	67	4	5.0	5.0	20	−11	1	4.5 to −4.5
4	F	60	20	3.0	4.5	21	−11	2	4.5 to −6
5	M	75	15	2.5	2.5	−20	−15	3	0 to −4.5
6	M	45	18	2.5	3.5	20	−9	3	6 to −4.5
Mean		63	13	3.3	3.8	20	−11	3	4 to −4

Stereotactic lesions are localized (in mm) with respect to the anterior commissure at the midline, as described in the atlas of Talairach (1993). Lesions were also localized along the anterior–posterior axis relative to the midpoint between the anterior (AC) and posterior (PC) commissures. The vertical extent of lesions are given as a range, since multiple lesions were placed.

gets repetitively for the duration of the 90-second PET scan. The targets were five Plexiglas dowels of 14-cm length, aligned vertically in a row and located 14 cm apart from each other. Each dowel was a different diameter, i.e., 90, 30, 48, 5, and 24 mm (from subject's left to right). The array was positioned over the subject at an optimal distance so that all targets could be easily grasped with the arm near full extension. Independent light sources were mounted within each dowel to specify which target should be grasped on each trial.

Patients were instructed to rest their left hand on their chest until one of the targets was illuminated (except Patient 5, right hand). Then, they were told to reach and grasp the sides of the illuminated dowel using a precision grasp, "as if the dowel were an egg or a delicate object." As soon as they had made contact with the object, they were to return to the starting position with the hand resting on the chest. One of the five targets was illuminated every 3 seconds and remained illuminated for 1.5 seconds. The first target appeared 9 seconds after the start of tracer injection and scanning. Twenty-seven trials were presented per scan. Targets appeared in random order across all trials. In the control task, patients were instructed to leave the left hand at rest on the chest and to look at each target as it was illuminated.

Subjects practiced the movement task for 5 minutes prior to the first PET scan. Movement and control tasks were performed in duplicate, in random order, for a total of four scans obtained prior to surgery and four scans after surgery.

Performance Measurements

The relative hand position was measured in 3 subjects with a Polhemus tracking device (Polhemus, Colchester, VT). A transmitter was taped to the dorsum of the patient's left hand and an antenna was located near the targets. The device samples the three orthogonal coordinates and three axes of rotation relative to the remote antenna at a frequency of 10 Hz. Data were collected for only the first 18 trials of each scan because of computer memory limitations.

Plots of spatial location versus time were graphically analyzed to determine the number of completed movement cycles, the total amount of movement time, and the duty cycle time (average time to complete one reach movement including the return to the starting position) during each scan. Because the Polhemus was limited to 10 Hz sampling and cannot be spatially calibrated near the scanner, more refined measures such as velocity or acceleration profiles were not derived.

Imaging Procedures

Images of rCBF were acquired using a modified autoradiographic method [15, 16]. For each scan, a bolus of 35 mCi of $H_2{}^{15}O$ was injected intravenously commensurate with the start of scanning and the behavioral task. A 90-second scan was acquired and reconstructed using calculated attenuation correction, with boundaries derived from each emission scan sinogram. Arterial blood samples were not obtained. Images of radioactive counts were used to estimate rCBF as described previously [17, 18].

PET images of rCBF were acquired with the Siemens 953/A tomograph. The device collects 31 contiguous planes covering a 105-mm field of view. The nominal axial resolution is 4.5 mm at full width half maximum (FWHM) and the transaxial resolution is 5.5 mm FWHM as measured with a line source. The tomograph was oriented 15 degrees steeper than the canthomeatal line, so the field of view did not include the orbitofrontal cortex.

MRI images of anatomy were obtained 3 to 6 days after the pallidotomy procedure with a 1.5-T GE Signa device or a Phillips Gyroscan device. A T1-weighted axial image set was acquired using the spin echo sequence: TE = 18, TR = 707 (voxel size = 0.82 × 0.82; slice thickness = 3–5 mm).

Imaging Analysis

Image processing was performed on a SUN 10/41 SPARC workstation. Postoperative MRI scans were digitally realigned parallel to the axis formed by the anterior and posterior commissures (AC and PC). Locations of both commissures along the midline were identified using the landmarks established by Talairach and Tournoux [19]. The location of each pallidal stereotactic lesion was visually identified and localized using Talairach coordinates. Because multiple electrocautery lesions were generated along the vertical tract of the stereotactic needle, the z-axis extent of each lesion is given as a range with respect to the AC-PC axis, rather than as a single site.

The statistical image analysis required all rCBF images to be aligned in a common stereotactic reference frame. Within-subject alignment of PET scans was performed using an automated registration algorithm [20]. The mean PET image from each individual was coregistered to the same subject's three-dimensional (3-D) volumetric MRI scan using another automated algorithm [21]. MRI and PET scans from the different patients were coregistered to a reference atlas centered in Talairach coordinates using an "affine" transformation with 12 degrees of freedom [19, 22, 23]. PET responses were localized in an orthogonal reference frame as defined by the Talairach stereotactic space [19]. Patient 5 had a pallidotomy in the left hemisphere. To match this patient to the other patients, the digital data from Patient 5 was flipped along the x axis so that the pallidotomy and rCBF responses would be on the right.

PET rCBF images were smoothed to a final isotropic resolution of 20 mm FWHM (as verified with a line source). For the given degree of image smoothing, the volume of this mask yielded approximately 92 gray matter resolving elements [24]. All smoothed images were normalized within subject using proportionate scaling calculated from the global activity of each scan.

Two-way analysis of variance (ANOVA) was used to identify significant effects and their interaction [25]. The two effects (and sources of variance) in the statistical model were *task* (movement or rest) and *treatment* (pre- and postpallidotomy). We were particularly interested in identifying significant *task–treatment* interactions at each location of the cortical–subcortical motor loop demonstrated in Figure 1. These would show areas with increased movement-related activity after pallidotomy. To correct for the multiple statistical comparisons for each of the sites in Figure 1, a statistical threshold of $p < 0.01$ was used.

An exploratory statistical analysis was also performed

across the whole brain to detect any additional areas showing statistical effects or interactions outside of our proposed model. In this case, a more stringent statistical threshold was set to reduce the likelihood of false positive results that can result from multiple independent comparisons. Since there were approximately 92 independent resolving elements for the degree of image smoothing, the threshold was set at $p < 0.0005$. Peak sites on the F-map above this threshold were localized and maximal F and p values and mean rCBF values were tabulated.

Results

Clinical Outcome and Pallidotomy Results

The stereotactic coordinates of each posteroventral pallidotomy are summarized in Table 1. Multiple lesions were placed along the vertical needle track in each procedure. Therefore, z-axis coordinates are given as a range with respect to the anterior–posterior commissural axis. The mean locations agree well with the target locations used by Laitinen: 18 to 21 mm lateral to the midline, 2 to 3 mm anterior to midcommissural point, and 3 mm below the anterior–posterior commissural axis [10]. The average location of the pallidotomy lesion is shown in Figure 2.

Clinical responses to pallidotomy in Patients 1 to 5 are described in a separate report [26]. In brief, patients with peak dose dyskinesias and dystonia showed improvement in dyskinesia rating scores. There was no improvement in Hoehn and Yahr and Unified Parkinson Disease Rating Scale (UPDRS) scores 8 weeks after surgery. All subjects were able to complete the PET functional imaging motor task before and after pallidotomy. There was no significant difference in the number of completed movement cycles, the total amount of movement time, and the duty cycle time after pallidotomy. Thus, differences in imaging results were not attributed to differences in total amount of movement or speed of movement.

Functional Imaging

Sites showing a significant treatment effect are summarized in Table 2. This was determined by contrasting all scans acquired preoperatively with scans acquired postoperatively. A marked reduction of rCBF after pallidotomy was localized to the posteroventral globus pallidus, as shown in Figure 2. Only three sites showed

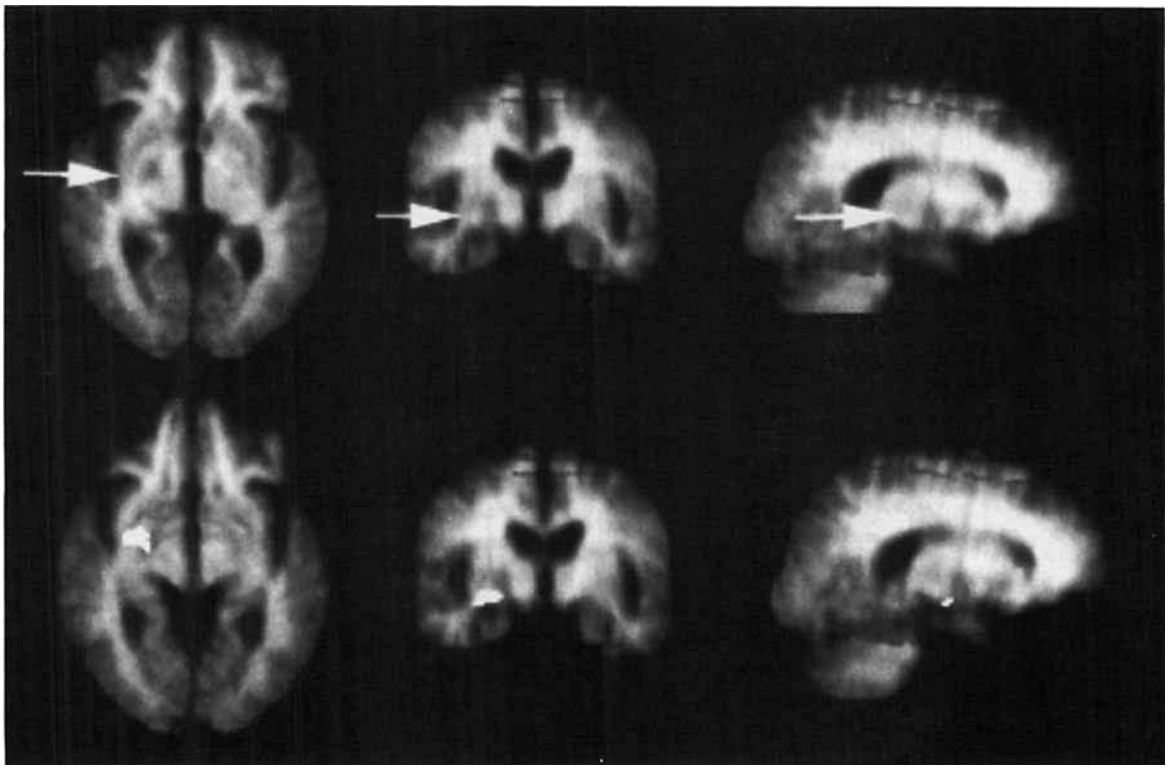

Fig 2. Localization of posteroventral pallidotomy. The images are a composite derived from the average of all 6 subjects after coregistration of magnetic resonance imaging (MRI) scans. MRI sections passing through the pallidotomy are shown in the upper row. The axial section is at the level of the anterior and posterior commissures (AC-PC) line, the coronal section is 11 mm posterior to the anterior commissure, and the sagittal section is 18 mm lateral to the midline. Arrows point to the average site of the pallidotomy. In the lower row the site with the maximal decrease of regional cerebral blood flow is in white superimposed on the average MRI. The axial section is 3 mm ventral to the AC-PC line; the sagittal and coronal sections are the same as in the upper row. Subjects' right is on the left side of the image.

Table 2. Treatment Effect after Pallidotomy

Anatomic Location	Talairach Coordinates			% of Increase of rCBF	ANOVA	
	x	*y*	*z*		*f*	*p*
Increased rCBF						
L parietal operculum	−54	−46	18	7.1	72.74	0.0004
L ventral motor	−59	−25	33	5.1	68.00	0.0004
L motor	−49	−30	46	7.4	68.71	0.0004
Decreased rCBF						
R globus pallidus	24	− 8	− 3	−6.5	44.88	0.001

Areas with a change of regional cerebral blood flow (rCBF) after pallidotomy. Coordinates are in millimeters with respect to the anterior commissure.

ANOVA = Analysis of variance; L = left; R = right.

increased activity with pallidotomy. All of the increases are in the hemisphere opposite to the stereotactic pallidotomy and include motor areas of the dominant hemisphere.

Areas showing significant task effect are summarized in Table 3. This was determined by contrasting all scans taken during movement with those taken at rest. Responses in motor effector areas are located in contralateral motor cortex, premotor cortex, and SMA. The locations of these sites with respect to the coregistered MRI anatomic reference are shown in Figure 3. The locations of responses are similar to results from normal subjects performing similar tasks [1, 14, 27, 28].

Areas with a significant task–treatment interaction are summarized in Table 4. This interaction identifies areas with a greater difference between movement scans and rest scans after pallidotomy. As hypothesized, the results include an augmentation of activity in the SMA and lateral premotor cortex. The locations of these sites are shown in Figure 4. These interactions remained significant ($p < 0.01$) even if the analysis excluded Subject 5. Unlike the other patients, this subject received a left pallidotomy and performed the task with the right hand. His imaging data were "flipped" between hemispheres along the lateral axis to match the other patients.

An additional site was located in the right anterior insula. This area is closely connected anatomically to premotor areas and may be an accessory motor area.

Discussion

The results confirm our hypothesis that pallidotomy increases movement-related activity in motor association cortex and provides additional evidence in support of a cortical basal ganglionic motor loop. Increases of movement related activity were located in both the SMA and premotor cortex after posteroventral pallidotomy. The observation supports the notion that motor behavior in PD is regulated via an interconnected cortical–basal ganglionic network that relies, in part, on thalamocortical facilitation. Although the results were only obtained in PD patients, it is probable that the same cortical–subcortical interactions are present in normal subjects. Our findings confirm and extend

Table 3. Task Effect: Movement Versus Rest

Anatomic Location	Talairach Coordinates			% of Increase of rCBF	ANOVA	
	x	*y*	*z*		*f*	*p*
R dorsal SMA	1	−28	55	3.6	59.05	0.0006
L ventral SMA	−15	−39	52	5.0	97.33	0.0002
R ventral SMA	14	−39	50	6.0	83.22	0.0003
R motor cortex	35	−44	45	8.3	42.83	0.002
L ventral premotor	−51	− 1	35	3.5	79.88	0.0003
R insula	35	−33	10	3.0	61.22	0.0005
L parietal operculum	−51	−19	7	2.5	83.04	0.0003
R ventral premotor	45	12	4	2.0	64.73	0.0005
R thalamus	23	−17	1	2.9	40.61	0.002

Changes of regional cerebral blood flow (rCBF) during left hand grasp task compared with control. Coordinates are in millimeters with respect to the anterior commissure.

ANOVA = Analysis of variance; R = right; SMA = supplementary motor area; L = left.

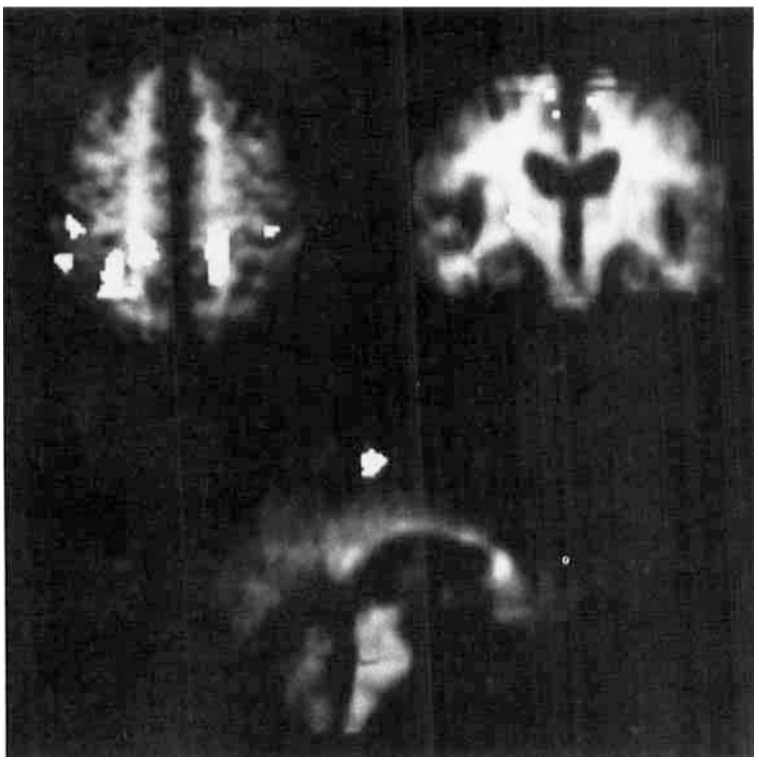

Fig 3. Movement-related responses in Parkinson's disease, using a left-hand prehension task. Significant increases of regional cerebral blood flow are shown in white, superimposed on the average magnetic resonance imaging scan from the group. The upper left axial section is 51 mm above the anterior and posterior commissures (AC-PC) line. Significant responses are located in motor cortex, premotor cortex, and ventral supplementary motor area (SMA). The upper right coronal section is 2 mm anterior to the vertical axis of the anterior commissure. A significant site is located in the ventral thalamus. The lower sagittal section is 2 mm right of midline. A significant response is located in the SMA. For axial and coronal sections the patient's left is on image right.

Table 4. Interaction of Pallidotomy and Movement

	Talairach Coordinates			ANOVA	
Anatomic Location	*x*	*y*	*z*	*f*	*p*
R premotor	20	−23	63	22.09	0.006
Ventral SMA	0	−15	55	34.51	0.002
R anterior insula	30	9	20	117.82	0.0001

Areas with greater movement-related activity (movement − rest) after pallidotomy. Coordinates are in millimeters with respect to the anterior commissure.

ANOVA = Analysis of variance; R = right; SMA = supplementary motor area; L = left.

a previous case report showing increased movement related activity of SMA in a patient with idiopathic PD who underwent pallidotomy and PET imaging [29]. Despite using different stereotactic localization, motor tasks, scanners, and image analysis methods, there is a clear concordance across laboratories in the functional outcome of pallidotomy in motor eloquent areas.

Our findings also suggest a modification of the cortical basal ganglia model proposed by Alexander and colleagues [3]. In their configuration, motor cortical areas were treated as a single entity. The imaging results suggest that human SMA and lateral premotor cortex are preferentially modulated by pallidothalamic inhibition compared with other areas such as primary motor cortex. The results also establish that it is possible to *predict* transsynaptic cortical increases of activity within highly specified neural circuits. The increased activity is behavior specific (e.g., movement versus rest). This approach is in sharp distinction to previous neuroimaging studies of "diaschesis," where transsynaptic decrements of brain activity, measured at rest, are observed after focal lesions [30].

One surprising effect of treatment was the increased activity in motor cortex opposite to the side of pallidotomy. This treatment effect is independent of the task patients were performing during imaging. One interpretation is that motor cortex opposite to subcortical lesions is preferentially recruited in a process of functional adaptation [31, 32].

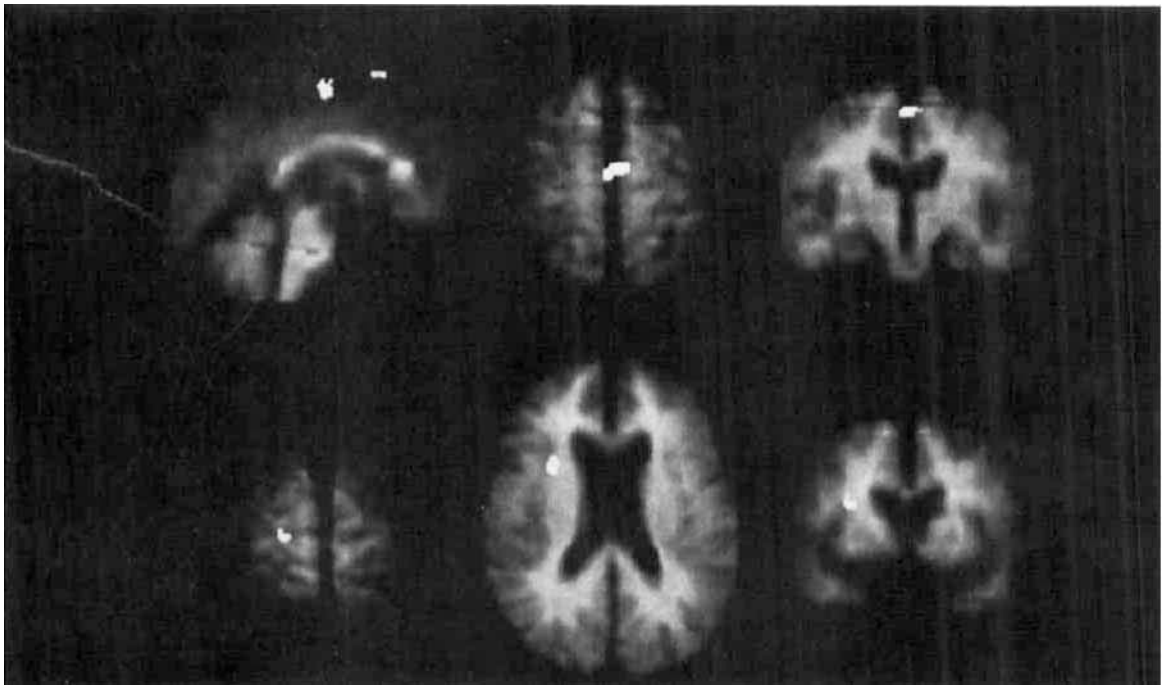

Fig 4. Interaction of pallidotomy and movement-related responses in motor cortex. Areas with a significant increase of movement-related activity after pallidotomy are shown in white, superimposed on the same subjects' average magnetic resonance imaging scans. The upper row shows the location of the supplementary motor area site in sagittal view at the midline, axial view 54 mm above the anterior and posterior commissures (AC-PC) line, and coronal section 15 mm behind the vertical axis of the anterior commissure. In the bottom row, the left hand axial section shows the location of the right premotor site 63 mm above the AC-PC line. The middle and right-hand picture show the location of a site in the anterior insular cortex. The axial section is 20 mm above the AC-PC line and the coronal section is 8 mm anterior to the vertical axis of the anterior commissure.

One major concern with this experimental design is whether the increased activity in the SMA and lateral premotor cortex is a behavioral artifact secondary to greater movement during imaging after the pallidotomy. This possibility is unlikely, as performance measurements revealed a nonsignificant difference in the number of movements and rate of movements before and after pallidotomy. Furthermore, from previous studies of the same task in normal subjects we have observed that changes in the number of movements or speed of movements best correlates with primary sensorimotor cortex [14]. However, in the present study the sensorimotor cortex showed no movement-related changes of activity. Therefore, the changes in SMA and premotor cortex are more likely related to an intrinsic modulation of activity in motor association areas related to the interruption of subcortical circuitry.

In the analysis of movement-related modulation of activity after pallidotomy, an additional area outside of the putative cortical–basal ganglia motor loop was identified in the right anterior insula (see Table 4). Changes in this site underscore the potential complexity of cortical–subcortical interactions in large-scale neural systems. In nonhuman primates the anterior insula has been shown to contain neurons with motor-related activity [33]. The site is closely interconnected with premotor areas and may represent a secondary motor area in humans.

Our findings reveal that motor planning and execution are not managed in isolation in motor cortical areas. Rather, it is the maintenance of cortical–subcortical connections that modulates movement. Although our patients had a significant increase of movement activity in motor association areas with pallidotomy, their overall clinical status and motor performance were not significantly enhanced with the surgical procedure [26]. The main clinical benefit was reduced dyskinesias and dystonia in a subset of the patients. We obtained our imaging results with a population-based analysis of PD patients and the localization method defines only those sites that are consistent across that population. With the relatively small number of subjects there are insufficient data to correlate reliably each individual subject's functional neuroimaging responses with clinical outcome and lesion localization. Thus, our results require cautious interpretation when extending the findings to individual patients. Additional studies are clearly needed to establish how small differences in lesion location modifies cortical activity

and functional outcome in PD. Ultimately, an understanding of the system's level interactions between cortical and subcortical motor areas may suggest prognostic features for functional recovery and rehabilitation strategies.

Supported in part by NS-01568 (S.G.) and a Human Frontiers Science Program award.

We thank Andrew Fagg for assisting in the acquisition of the performance data, Steven Hayles for technical support, Lou Mallory for recruiting patients, and Roger Woods, MD, for kindly providing registration software.

References

1. Playford ED, Jenkins IH, Passingham RE, et al. Impaired mesial frontal and putamen activation in Parkinson's disease: a positron emission tomography study. Ann Neurol 1992;32:151–161
2. Rascol O, Sabatini U, Chollet F, et al. Supplementary and primary sensory motor area activity in Parkinson's disease. Regional cerebral blood flow changes during finger movements and effects of apomorphine. Arch Neurol 1992;49:144–148
3. Alexander GE, Crutcher MD, DeLong MR. Basal ganglia thalamo-cortical circuits: parallel substrates for motor, oculomotor, "prefrontal" and "limbic" functions. Prog Brain Res 1990;85:119–146.
4. Bergman H, Wichmann T, DeLong MR. Reversal of experimental Parkinsonism by lesions of the subthalamic nucleus. Science 1990;249:1436–1438
5. DeLong MR. Primate models of movement disorders of basal ganglia origin. Trends Neurosci 1990;13:281–285
6. Bergman H, Wichmann T, Karmon B, DeLong MR. The primate subthalamic nucleus. II. Neuronal activity in the MPTP model of Parkinsonism. J Neurophysiol 1994;72:507–520
7. Wichmann T, Bergman H, DeLong MR. The primate subthalamic nucleus. III. Changes in motor behavior and neuronal activity in the internal pallidum induced by subthalamic inactivation in the MPTP model of Parkinsonism. J Neurophysiol 1994; 72:521–530
8. Sterio D, Beric A, Dogali M, et al. Neurophysiological properties of pallidal neurons in Parkinson's disease. Ann Neurol 1994;35:586–591
9. Jenkins IH, Fernandez W, Playford ED, et al. Impaired activation of the supplementary motor area in Parkinson's disease is reversed when akinesia is treated with apomorphine. Ann Neurol 1992;32:749–757
10. Laitinen LV, Bergenheim AT, Hariz MI. Leksell's posterventral pallidotomy in the treatment of Parkinson's disease. J Neurosurg 1992;76:53–61
11. Grafton ST, Sutton J, Couldwell W, et al. Network analysis of motor system connectivity in Parkinson's disease. Modulation of thalamocortical interactions after pallidotomy. Hum Brain Mapping 1994;2:45–55
12. Raczkowski D, Kalat JW. Reliability and validity of some handedness questionnaire items. Neuropsychologia 1980;18:213–217
13. Couldwell WT, Apuzzo MLJ. Initial experience related to the use of the Cosman-Roberts-Wells stereotactic instrument. J Neurosurg 1990;72:145–148
14. Grafton ST, Fagg AH, Woods RP, Arbib MA. Cortical control of prehensile movements in humans. Cereb Cortex 1995 (In Press)
15. Herscovitch P, Markham J, Raichle ME. Brain blood flow measured with intravenous $H_2{}^{15}O$. I. Theory and error analysis. J Nucl Med 1983;24:782–789
16. Raichle ME, Martin WRW, Herscovitch P. Brain blood flow measured with intravenous $H_2{}^{15}O$. II. Implementation and validation. J Nucl Med 1983;24:790–798
17. Fox PT, Mintun MA, Raichle ME, Herscovitch P. A noninvasive approach to quantitative functional brain mapping with $H_2{}^{15}O$ and positron emission tomography. J Cereb Blood Flow Metab 1984;4:329–333
18. Mazziotta JC, Huang S-C, Phelps ME, et al. A noninvasive positron computed tomography technique using oxygen-15-labeled water for the evaluation of neurobehavioral task batteries. J Cereb Blood Flow Metab 1985;5:70–78
19. Talairach J, Tournoux P. Referentially oriented cerebral MRI anatomy. New York: Thieme Medical, 1993
20. Woods RP, Cherry SR, Mazziotta JC. Rapid automated algorithm for aligning and reslicing PET images. J Comp Assist Tomogr 1992;115:565–587
21. Woods RP, Mazziotta JC, Cherry SR. MRI-PET registration with automated algorithm. J Comp Assist Tomogr 1993;17: 536–546
22. Woods RP, Mazziotta JC, Cherry SR. Automated image registration. Ann Nucl Med 1993;7(suppl):S70 (Abstract)
23. Grafton ST, Woods RP, Tyszka JM. Functional imaging of procedural motor learning: relating cerebral blood flow with individual subject performance. Hum Brain Mapping 1994;1:221–234
24. Worsley KJ, Evans AC, Marrett S, Neelin P. A three-dimensional statistical analysis for CBF activation studies in human brain. J Cereb Blood Flow Metab 1992;12:900–918
25. Neter J, Wasserman W, Kutner MH. Applied linear statistical models. Boston: Irwin, 1990
26. Sutton JP, Couldwell W, Lew MF, et al. Ventroposterior medial pallidotomy in patients with advanced Parkinson's disease. Neurosurgery 1995 (In Press)
27. Deiber M-P, Passingham RE, Colebatch JG, et al. Cortical areas and the selection of movement: a study with PET. Exp Brain Res 1991;84:393–402
28. Grafton ST, Mazziotta JC, Woods RP, Phelps ME. Human functional anatomy of visually guided finger movements. Brain 1992; 115:565–587
29. Ceballos-Baumann AO, Obeso JA, Vitek JL, et al. Restoration of thalamocortical activity after posteroventral pallidotomy in Parkinson's disease. Lancet 1994;344:814
30. Baron JC, Bousser MG, Comar D, Castaigne P. Crossed cerebellar diaschisis in human supratentorial brain infarction. Trans Am Neurol Assoc 1981;105:459–461
31. Chollet F, DiPiero V, Wise RJS, et al. The functional anatomy of motor recovery after stroke in humans: a study with positron emission tomography. Ann Neurol 1991;29:63–71
32. Weiller C, Chollet F, Friston KJ, et al. Functional reorganization of the brain in recovery from striatocapsular infarction in man. Ann Neurol 1992;31:1463–1472
33. Preuss TM, Goldman-Rakic PS. Connections of the ventral granular frontal cortex of Macaques with perisylvian premotor and somatosensory areas: anatomic evidence for somatic representation in primate frontal association cortex. J Comp Neurol 1989;282:293–316